GEOPHYSICS, VOL. 68, NO. 1 (JANUARY-FEBRUARY 2003); P. 58–69, 7 FIGS.
10.1190/1.1543194

Case History

Controls on acoustic properties of Upper Jurassic siliciclastic rocks (Boulonnais, northern France)

Hendrik Braaksma*, Jeroen A. M. Kenter*, Jean Noel Proust‡, Vincent Dijkmans*, Tomas van Hoek*, Geoffroy Mahieux**, and Guy G. Drijkoningen§

ABSTRACT

More than 200 plugs from outcrop and a nearby borehole in a carbonaceous siliciclastic interval of Late Jurassic (Kimmeridgian to Tithonian) age were quantitatively analyzed for texture, mineralogy, and acoustic properties. Our primary goal was to study the effect of clay (fraction smaller than 8 μm), silt/sand (fraction larger than 8 μm), and carbonate on the acoustic properties. The quantitative nature and volume of the data made it possible to observe four-dimensional relationships in contoured ternary diagrams. Primary control on the acoustic properties is exerted by porosity, but the trend of this relationship significantly deviates from popular velocity transforms. The contribution of clay, silt/sand, and carbonate particular material and cement explains the remaining variation in acoustic properties. Although no clear linear thresholds are defined, a general trend is that clay and carbonate content have opposite and overlapping effects on acoustic properties, the influence of clay content progressively increases with decreasing carbonate content, and visa versa. With increasing carbonate content, the variation of acoustic velocity at a given porosity value increases to nearly twice of that in the clay-dominated sediment. Traditional classification boundaries are present but strongly overprinted by this interplay between clay and carbonate.

This study may have important implications for porosity and lithofacies prediction from wireline logs in similar mixtures of sediment. In addition, the quantitative character of the textural and mineralogical data may provide a direct link from acoustic properties to the primary depositional system and sequence stratigraphy.

INTRODUCTION

The complex relationship between acoustic properties and lithofacies of sedimentary rocks strongly influences the seismic response and seismic stratigraphic interpretation of seismic reflection data. As a consequence, seismic images are nonunique and require continuous calibration and ground truthing by geology. Correlation and calibration of geological parameters and petrophysical properties that control the seismic response of sedimentary packages is a first step to investigate this relationship. Boreholes provide in situ measurements of acoustic properties, density, and velocity, at various frequencies and scales. However, they lack the spatial attributes of the depositional system that controls the mineralogical and textural composition and diagenetic history of the rocks.

Siliciclastics traditionally have been the primary target of research on the acoustic properties of sedimentary rocks because of their importance in petroleum exploration. Since the late 1950s, numerous papers have been published on the elastic properties of siliciclastic sediments (sandstone and shale) and have resulted in some widely used empirical and experimental velocity transforms. For example, the time average equation of Wyllie et al. (1956) relates velocity to porosity in saturated and consolidated sediments, and the experimental relationship

Manuscript received by the Editor April 26, 2001; revised manuscript received July 8, 2002.
*Vrije Universiteit Amsterdam, Department of Earth and Life Sciences, De Boelelaan 1085, 1081 HV Amsterdam, Netherlands. E-mail: brah@geo.vu.nl; kenj@geo.vu.nl.
‡Université de Rennes 1, Géosciences, Campus Beulieu, bat. 15, 35042 Rennes Cedex, France.
**Université de Picardie Jules Verne, Departement de Geologie, 33 rue Saint-Leu, 80039 Amiens Cedex, France.
§Delft University of Technology, Department of Applied Earth Sciences, Mijnbouwstraat 120, 2628 RX Delft, Netherlands.

by Gardner et al. (1974) correlates density and velocity for a variety of rocks. Numerous modifications of especially the time-average expression were published to adjust for deviations within real data sets and to include physics-oriented solutions that incorporate the internal rock structure (Nafe and Drake, 1963; Raymer et al., 1980; Wang and Nur, 1992; Dvorkin and Nur, 1998). Although these expressions explain velocity-density and velocity-porosity relationships in discrete data sets with relatively uniform texture and mineralogy, they do not adequately predict relationships in mixed clastic, pure carbonate, and mixed clastic-carbonate data. In addition, they fail to explain trends in large data sets composed of mixed lithologies from different geographic locations.

Several attempts have been made to document the influence of mixed mineralogy on acoustic velocities. For example, Tosaya and Nur (1982), and Kowallis et al. (1983) demonstrated for water-saturated siliciclastic sediments the relationship between sonic velocities and porosity or clay content. Vernik and Nur (1992) translated this into the effect of sediment fabric on the acoustic velocity in mixtures of clay and sand. Stafleu et al. (1994) confirmed the clay effect on the sonic velocity of tight carbonates; they showed a critical threshold of 5–8% clay that inversely affects velocity. Kenter et al. (1997b) quantified the effect of quartz content on the velocities of carbonates.

This study is an attempt to quantitatively relate measurements of acoustic properties to parameters such as clay, silt, quartz, and carbonate content that can be linked to lithofacies and, ultimately, to the depositional system. Plug samples were drilled from a freshly weathered cliff face and whole core derived from a nearby borehole. Along with measurements of mineralogy and grain size, this provided the data for the link with geological parameters, a comparison among core and cliff acoustic properties and, finally, with published velocity transforms. The research is part of two linked projects, Integrated Solid Earth Sciences (ISES) and "Projet Image Sismique et Sédiments", integrating geophysics, petrophysics, and geology from subsurface and nearby continuously exposed cliffs. The link of the acoustic properties to the depositional system as well as the integration of reflection seismics, borehole geophysics, and petrophysics are the subjects of research papers that will follow.

GEOLOGIC SETTING

The selected data set is from the upper Jurassic in the Boulonnais, northern France, and consists of an alternation of intervals dominated by shale, sandstone, and carbonate exposed in a freshly weathered coastal cliff face (Figure 1). The depositional setting ranges from shallow marine offshore shales to shoreface sandstone deposits with varying amounts of carbonate and has been thoroughly studied (e.g., Geyssant et al., 1993; Herbin et al; 1993; Proust et al., 1993, 2001; Mahieux et al., 1998, 1999). This report focuses on a 100–120 m thick interval of mixed siliciclastic-carbonate deposits, exposed below the Cap de la Crèche, directly south of Wimereux (Figure 1b). The studied interval in the cliff and subsurface is generally subdivided into three sandy formations (Grès de Conninc-thun, Grès de Châtillon, Grès de la Crèche), three shale- and mudstone-dominated formations (Argiles de Moulin Wibert, Argiles de Châtillon, Argiles de la Crèche), and one argillaceous limestone (Calcaires du Moulin Wibert) (Figure 1c). The spatial variation of lithofacies units is attributed to effects of eustacy on a very low-angle siliciclastic-dominated depositional ramp (Mahieux et al., 1998; 1999; Proust et al., 2001). The Boulonnais sections represent a landward time-equivalent of the offshore marine source rocks deposited around the London swell in the North Sea (Cornford, 1984; Williams, 1986) and in basins as distant as western Siberia. In the Dover Strait, the Kimmeridge Clay, with petroleum potential of up to 20 kg of hydrocarbons per ton of rock (kg HC/t), consists of five horizons of shales interbedded with calcareous sandstone (Gallois, 1976).

METHODS

Acoustic properties

Nearly 170 1.5-inch and 1.0-inch diameter core plugs for petrophysical analyses were drilled at 30-cm intervals along a measured section (Figure 1b). The plugs, vertically and/or horizontally orientated with respect to the bedding, were drilled with 1.5-inch or 1.0-inch diamond dust–coated drill bits. After the removal of the plugs from the outcrop, they were wrapped in plastic foil to prevent drying and placed in a PVC tube to avoid breakage. The tubes were then stored in a cooler to prevent loss of water. Clean sands are underrepresented in the grain-size data set and absent from the plug data because the unconsolidated state, or lack of carbonate cement of these sands, did not allow proper sampling. A total of 61 plugs were drilled from whole core in the equivalent section derived from a 120-m deep borehole drilled on a nearby beach, some 1500 m away from the cliff section.

Upon arrival in the laboratory, all plugs were cut to a maximum length of 5 cm and subdivided into predominantly shaley or calcareous to sandy lithologies. This separation was made because the shaley plugs, which are soft and friable, require different sample preparation than the more resistant plugs of calcareous to sandy lithologies. Next, the sample ends of the more resistant plugs were ground flat and parallel to within 0.001 inch (0.025 mm), the plugs were saturated with seawater (35 promille) and stored under vacuum for 48 hours. The shaley plugs were cut with a sharp knife and carefully rewrapped to preserve moisture.

Ultrasonic compressional (P-wave) and shear wave (S-wave) velocities were measured as a function of pressure using a transducer arrangement (Verde Geosciences, Vermont) that propagated a compressional (V_p) and two independent and orthogonally polarized shear waves (V_{s1} and V_{s2}) along the core axis. A source crystal was excited by a fast rise-time electrical voltage pulse, producing an ultrasonic pulse with a frequency of 500 kHz, which was recorded by a receiver crystal. Measuring the one-way traveltime of the acoustic wave along the sample axis and dividing by the sample length produced the acoustic velocities. The arrival time of the one-way traveltime was picked when the signal exceeded a threshold voltage equal to 3% of the overall peak-to-peak amplitude of the first three half cycles of the signal. Precision of the measured velocities is within approximately 5% (when coupling between source- and receiver crystal and core-plug were sufficient). Obscure measurements were not used for further analyses. The measurements were generally conducted at five effective pressures ranging from 0 up to 30 MPa. Because pore pressure was kept at 0 MPa, the effective pressure in this experiment was equal to

the confining pressure. Common values for confining pressures were 0, 2.5, 5, 7.5, 10, and 15 MPa, some of the more coherent plugs were measured at confining pressures up to 30 MPa.

Following the acoustic measurements, bulk (saturated) density and porosity were measured. Plugs were weighed and dried for at least 72 hours at 70°C. Next bulk and dry densities were calculated from wet and dry sample weights and measured cylinder volumes. Grain densities were derived by dividing the mass of the powdered samples by the volume using a Micrometrics AccuPyc 3200 helium pycnometer. This procedure provides an accuracy of 0.03%. Total porosity was calculated from dry and grain density. More detailed procedures are described by Carmichael (1990), Kenter and Ivanov (1995), and Bracco Gartner et al. (1997).

Grain size and carbonate content

In addition to subsamples of the 228 cylindrical plug samples, 259 samples were collected for the analysis of grain size and carbonate content. Grain size was measured using a Fritsch A22

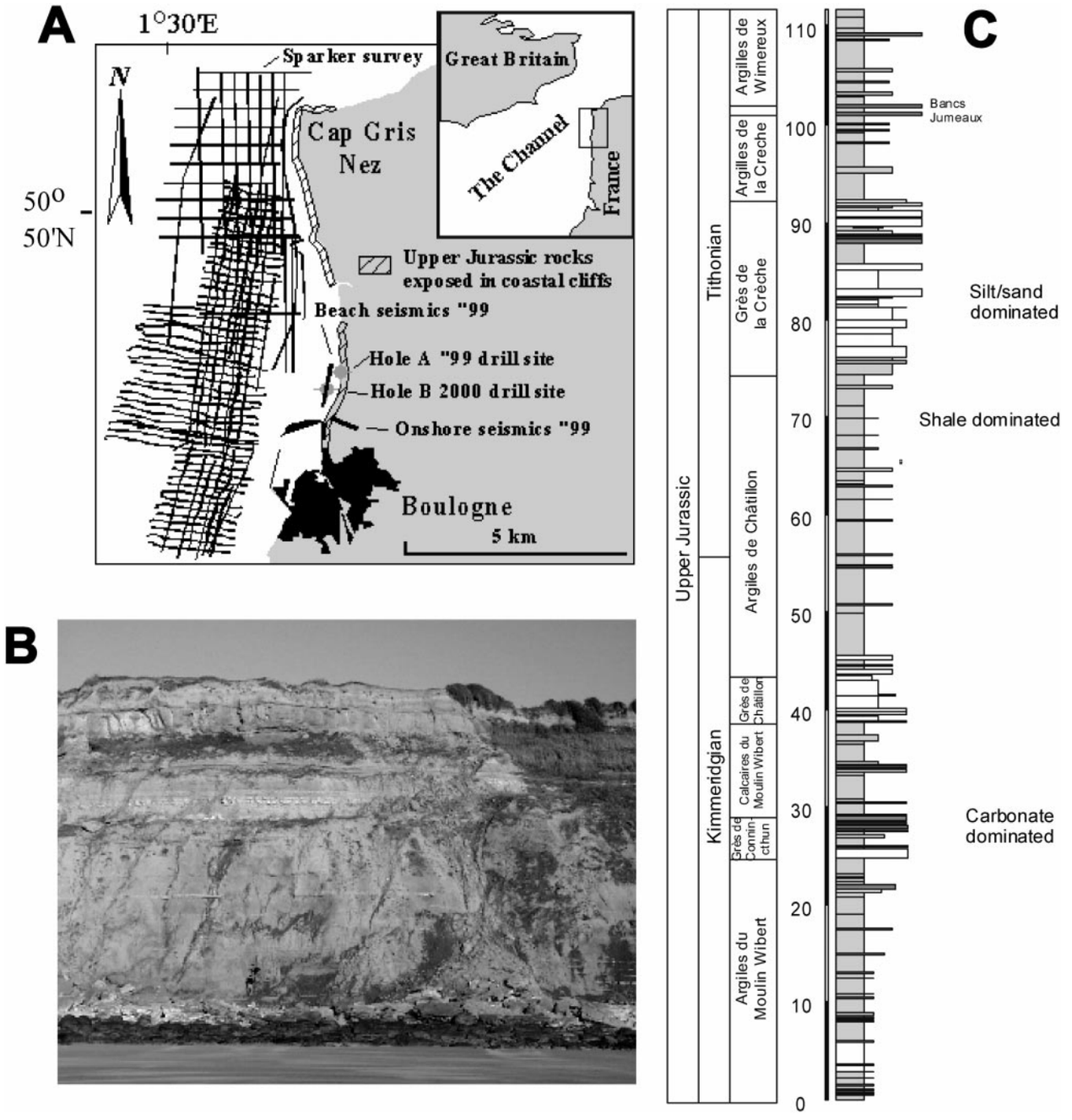

FIG. 1. Location map of cliff section, and borehole, (a) photo of cliff simplified lithologic log with lithologic units (b). See people for scale.

Laser Diffraction Spectrophotometer or "Laser Particle Sizer," which has a working range of 0. 16–1400 μm. The analytical procedure is based on the forward light diffraction of the laser beam by the sediment particles. Single particles are regarded as two-dimensional objects and grain size is measured as a function of the cross-sectional area of that particle. The following assumptions are made. (1) The transformation of diffraction patterns to grain sizes is based on matrices, which are calculated for spheres. As a consequence, the diffraction along the cross-sectional area of the particle is attributed to the diffraction of spheres. (2) Grain orientation is assumed to be randomly distributed. Often, however, measurements take place in a continuous flow of particles in which the particle may be orientated with respect to its shape (Konert and Vandenberge, 1997). The resulting volume percentage measurements were reduced to the following frequency classes: clay (<8 μm), silt (8–63 μm), and sand (>63 μm) using the Udden-Wenthworth grain-size scale (Prothero and Schwab, 1996). The upper limit for clay fraction was set at 8 μm as a consequence of the measuring technique. Konert and Vandenberge (1997) have documented that the assumption of spherical particles introduces a considerable error when measuring platy clay minerals, and that grain sizes <2 μm measured with the pipette method correspond with a grain size of 8 μm defined by the Laser Particle Sizer.

Prins and Stuut (1999) reported on the discrepancy between the actual weight percentages of the grain-size distribution and the volumetric grain-size distribution measured. They concluded that the Laser Particle Sizer underestimates the volume percentage of blocky particles (e.g., quartz) compared to relatively nonspherical or platy particles (e.g., clay minerals) in sediment standards. In addition, they showed that the discrepancy generally increases with increasing grain size. Since a large part of the data set consists of shale, the problem was ignored.

Carbonate measurements followed the Scheibler procedure (Kenter et al., 1997b). The weight percentage of carbonate is calculated from the carbon dioxide volume. Grain-size fractions and volume percentages were converted to fractional weight percentages assuming that the associated error is minimal. The assumption is made that the 8-μm threshold measured by the Laser Particle Sizer separates clay particles from granular quartz grains and reflects a crucial difference in petrophysical behavior. As a result, the following textural-mineralogical fractions are distinguished: carbonate (granular and cement combined), clay (<8 μm), and silt/sand (>8 μm). These groups represent not only a difference in grain size but also in mineralogy.

RESULTS

Acoustic properties

Maximum P-wave velocities are reached at confining pressures of 4.0–5.0 MPa, after which only minimal increase of velocity was observed (Figure 2). As a consequence, the velocities at 10 MPa are regarded as terminal velocities (Bourbié et al., 1987). No information on the maximum overburden of the Upper Jurassic interval is available from the literature. It is estimated from reconstruction of the regional geology that the overlying sediment package may have reached a thickness of no more than 500 m (El Albani et al., 1993). This would translate in a confining pressure of up to 10–15 MPa before erosion. The observed shale velocities of approximately 2.0 km/s correspond well with the velocity-depth relationship published by Jankowsky (1970).

P-wave velocities in the total data set range from slightly under 2.0 to nearly 6.0 km/s, whereas *S*-wave velocities range between 0.7 and 3.3 km/s (Figures 3a and 3b). Porosity ranges from 2% to 41%, and density ranges between 2.0 and 2.7 g/cm^3. P-wave velocity displays a general, nearly linear decrease in velocity with increasing porosity up to nearly 20% (Figure 3c). In this interval, velocity has a range of approximately. 1 km/s at one given porosity value. Between 20% and 40% porosity, velocity shows a minor decrease and a variation in velocity of about 0.5 km/s at a given porosity value. No shear wave velocities were measured in the core-derived data since the quality of the arrivals was obscure. Minor differences exist between cliff and core plug samples. Only at densities higher than 2.3 g/cm^3 or fractional porosities below 0.23 are P-wave velocities from core plugs some 10% higher compared to those of the cliff-derived plugs.

Ternary diagrams linking acoustic, mineralogical, and textural properties

In order to relate the acoustic properties to geological parameters that, in turn, can be linked to the depositional system, the mineralogical, textural, and acoustic properties were plotted in ternary diagrams. Quartz silt and sand fractions as well as minor contributions by feldspar were combined because they

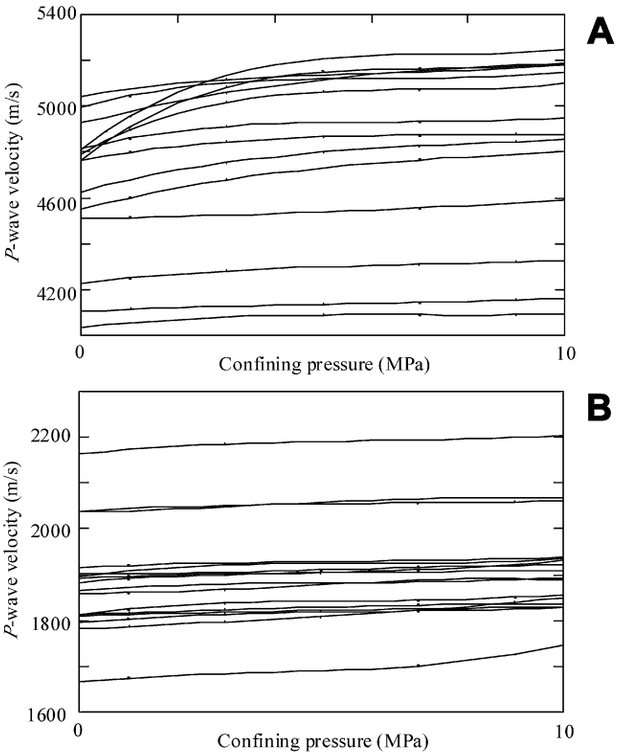

FIG. 2. Crossplots of P-wave velocity as a function of confining pressure for a selected number of plug samples of predominantly poorly lithified shaley (a) and sandy to carbonaceous (b) composition. See text for discussion.

are granular materials that are expected to have comparable mechanical and elastic behavior, as opposed to clay particles, which are platy and have cohesive forces.

The textural and mineralogical composition of the total data set and that of the plugs, clay, silt/sand, and carbonate were plotted in a ternary diagram. Next, the total number of data points was recorded in windows measuring 10% of each component (shown in the background of diagram in Figure 4), where common points were weighed between bordering triangles. Finally, the values were converted to fractions of the total amount of data points and contoured. Figure 4 shows the ternary diagrams for the total data set of 487 samples (Figure 5a) and for the 228 plug samples (Figure 5b). The total data set clearly shows a compositional continuum between clay, silt/sand, and carbonate. However, there is predominance for equal mixtures of silt/sand and clay with carbonate contents below 40%, or calcareous shales to silt/sandstone. Another concentration is observed at carbonate contents over 60% with minor clay and silt/sand fractions, or argillaceous carbonates. Remarkable is the absence of sediments that are mixtures of clay and carbonate. Apparently, these mixtures are not produced in this particular depositional system.

To display the quantitative relation between sediment composition and acoustic properties, acoustic velocity, density,

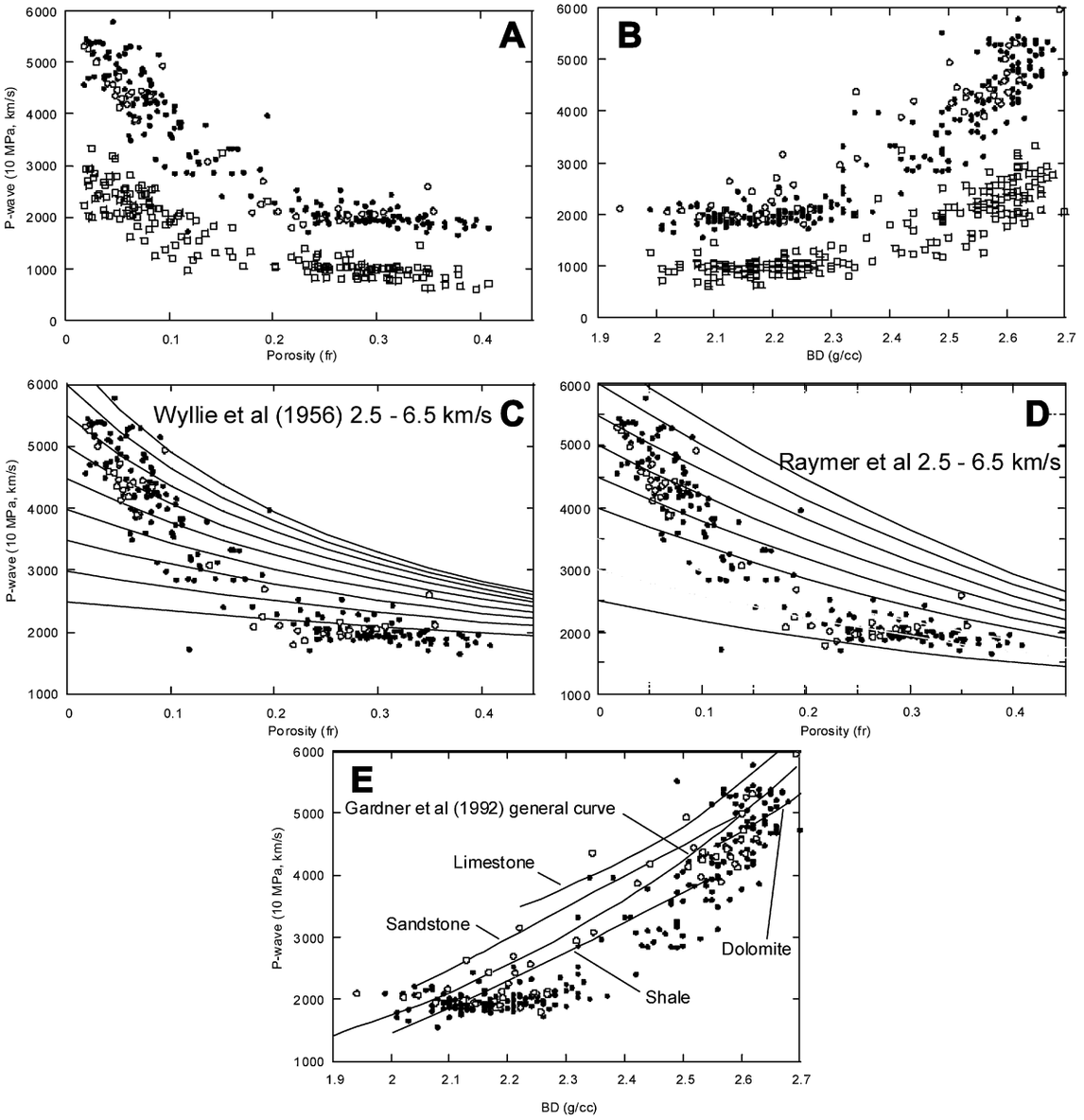

FIG. 3. Crossplots of terminal water-saturated P- and S-wave velocities versus density (a) and porosity (b) for the total data set of 228 plug samples. General velocity expressions such as the time average expression (Wyllie et al., 1956), the Raymer equation (Raymer et al., 1980) and Gardner's empirical experimental equation (Gardner et al., 1974) are added to the data in, respectively, (c), (d), and (e). P-wave and S-wave velocities for cliff-derived plug samples are respectively represented by solid circles and open squares; P-wave velocities for the core plugs are open circles. See text for discussion.

porosity, and impedance were plotted as a function of their composition (Figure 5). The resulting values were averaged in windows measuring 10% of each ternary component (shown in the background of diagram in Figure 5), where common points were weighed between bordering triangles and contoured. Figure 5a through Figure 5d clearly demonstrate that the petrophysical properties are a function of all three combined textural and mineralogical parameters. Three areas are observed in the porosity distribution: porosities lower than 5–10% for mixtures dominated by carbonate and silt/sand, porosities between 10 and 30% for mixtures of carbonate and silt/sand with clay contents between 1% and 30%, and porosities over 30% for mixtures with silt/sand over 80%, clay over 30–50% (Figure 5a). Bulk density shows a subdivision in two areas: for carbonate contents higher than the 15–60% line bulk density decreases rapidly from 2.55 to 2.2 g/cm^3, primarily as a function of increasing clay content, and an area with bulk densities between 2.0 and 2.2 g/cm^3, where clay and silt/sand dominate and carbonate falls below the 15–60% line (Figure 5b).

Sonic velocity displays a slightly more irregular distribution: velocities higher than 4.0 km/s for mixtures of carbonate and silt/sand with clay contents lower than 10–20%, velocities between 1.8 and 2.0 km/s for mixtures of clay and silt/sand with carbonate content below a 50–15% line, and an transitional zone where velocities rapidly decrease from 4.0 to 2.0 km/s (Figure 5c). Impedance shows a comparable distribution: impedance values of 9.0–12.0 $\times$ 10^6 kg/m^{2}s for mixtures of carbonate and silt/sand with clay content lower than 10–25%, and "flat" area with impedance values between 4.0 $\times$ 10^6 and 4.5 $\times$ 10^6 kg/m^{2}s dominated by clay, and an intermediate area of rapidly decreasing impedance with increasing clay content. Because not only the absolute values of sonic velocity and impedance are a function of clay, carbonate, and silt/sand contents, also their range is affected. The latter was contoured in Figures 5e and 5f. Because a significant number of cells (triangles shown in the background) have only one value and the average number of observations per cell is 2.3, no standard deviations were calculated. Although this affects the statistical strength, still several important observations can be made that have implications for the prediction of physical parameters in similar data sets. First, the range in velocity is significantly higher (more than 2.5 km/s) for mixtures where clay content is more than 10–20%, whereas in the remaining area the range is almost 50% of this (Figure 5e). Second, the range in impedance similarly is nearly twice that in mixtures of carbonate and silt/sand with clay contents below 20% and carbonate over 20% than in mixtures dominated by clay and/or more than 75% silt/sand (Figure 5f).

Figures 6a–6d show typical examples of mixtures of silt/sand and carbonate with low clay content and, consequently, velocities more than 3.5 km/s and impedance values more than 9 $\times$ 10^6 kg/m^{2}s. Though quartz content ranges from nearly zero to more than 90% and textural properties (shape of quartz grains) as well as packing varies considerably, the low clay contribution and the presence of carbonate explains the high but variable sonic velocities and impedance. Figures 6e and 6f show examples of mixtures with comparable amounts of carbonate but in addition high amounts of clay. Here, velocities and impedance values are lower, but still 2.5–3.5 km/s[1] and 4.5–6.0 $\times$ 10^6 kg/m^{2}s, respectively, probably as the result of the diagenetic effect of the present carbonate (cement). Low velocity and impedance mixtures with minor variation in values are shown in Figures 6g–6k. Sediments are fine grained and dominated by clay and silt/sand with low amounts of carbonate (carbonaceous shales), most of which is probably fine peloidal grains with minor cement. Finally, Figure 6l shows a shale with clay content of 50% and low velocity and impedance.

DISCUSSION

Overburden and microcracks

Density values, between 2.0 and 2.35 g/cm^3, and acoustic velocities between 1.8 and 2.2 km/s of the shale samples suggest burial depths far less than 1 km (e.g., Domenico, 1977; Kopf, 1979). This is in good agreement with the estimated approximately 500-m overburden derived from geological reconstruction.

Though it is assumed that effective pressures of 40 MPa or more are required to close cooling or stress-relief induced microcracks (Vernik and Nur, 1992), no significant increase of velocity was observed at pressures above 10 MPa (Figure 2). It is therefore assumed that microcracks are either closed at

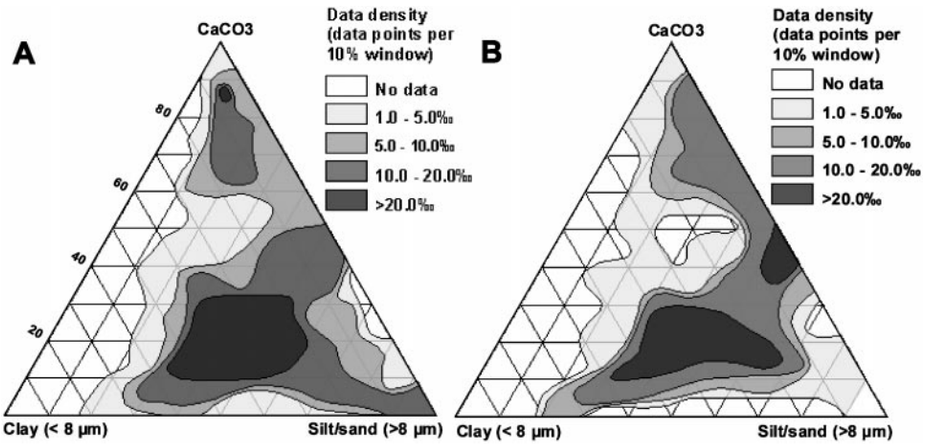

FIG. 4. Ternary diagrams showing the contribution of clay, silt/sand, and carbonate content for the entire data set of 487 plug samples and spot samples (a) and for plug samples only (b). See text for discussion.

these pressures or, if they still exist, do not obscure the acoustic measurements.

Velocity transforms—Comparison

Neither the time average equation (Wyllie et al., 1956) nor the Raymer expression (Raymer et al. 1980) for various rock matrix velocities can adequately explain the observed trends in the high-velocity range (Figures 3c and 3d). They do, however, closely follow the low-velocity variation between porosity and velocity. In density-velocity space, the various Gardner curves (Gardner et al., 1974) do not follow the trend of the data well (Figure 3e). Although Vernik and Nur (1992) use sediment fabric in siliciclastics as a key parameter to explain secondary

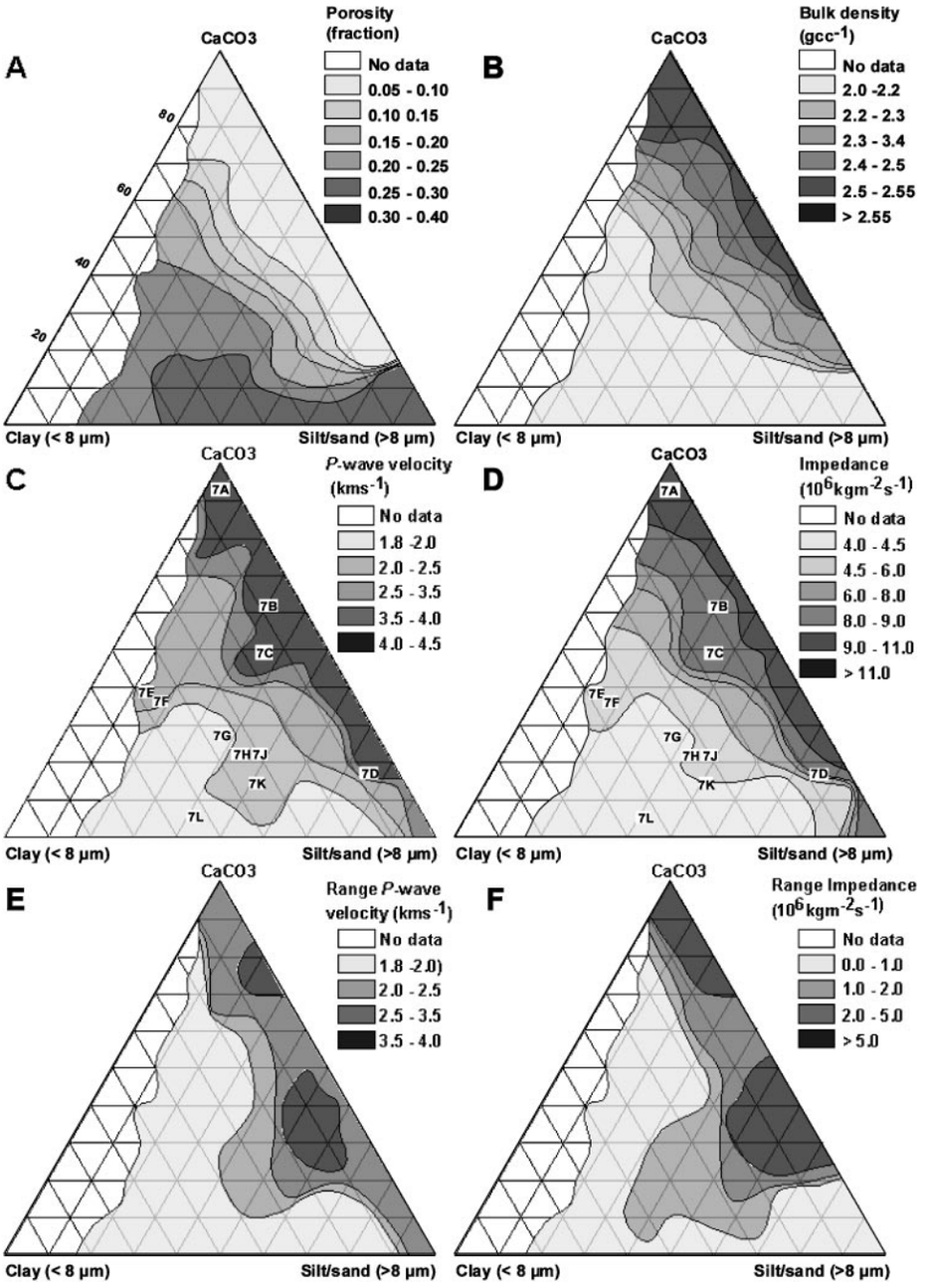

FIG. 5. Ternary diagrams showing the relationships between fractional porosity (a), bulk density (b), P-wave velocity (c), impedance (d), and textural and mineralogical compositions for the 228 plug samples. Compare with Figure 4 for data distribution. (e) and (f) display ternary diagrams with contours of the range of P-wave velocity and impedance, respectively. It must be noted that these diagrams lack statistical strength since a substantial number of triangles have only one data point. However, they still show important relationship that can also be observed in Figures 7a and 7b. The number of samples is 228. Symbols in Figure 5c relate to photomicrographs shown in Figure 6. See text for discussion.

trends in velocity-density space, their approach is semiquantitative rather than quantitative.

Clearly, the trends and variation at one specific density or porosity value cannot be explained by the existing velocity equations. Figure 7 shows various crossplots of mineralogical and textural properties versus acoustic velocity. Both clay and carbonate content show abrupt thresholds that affect the P-wave velocity. As the clay content increases from 0 to approximately. 12%, velocity shows a steep decrease; as the clay content increases further, there is hardly any change observed in velocity values (Figure 7a). Similarly, carbonate contents between 0 and 40% correspond to low acoustic velocities with minor variation. At 40%, however, velocities and their range at a given porosity value increase dramatically (Figure 7b). Clay content shows opposing linear relationships with porosity and density (Figures 7c and 7d), because these clays not only have a higher textural porosity but also bear water in the molecular structure. Apparently, the porosity reduction as a result of

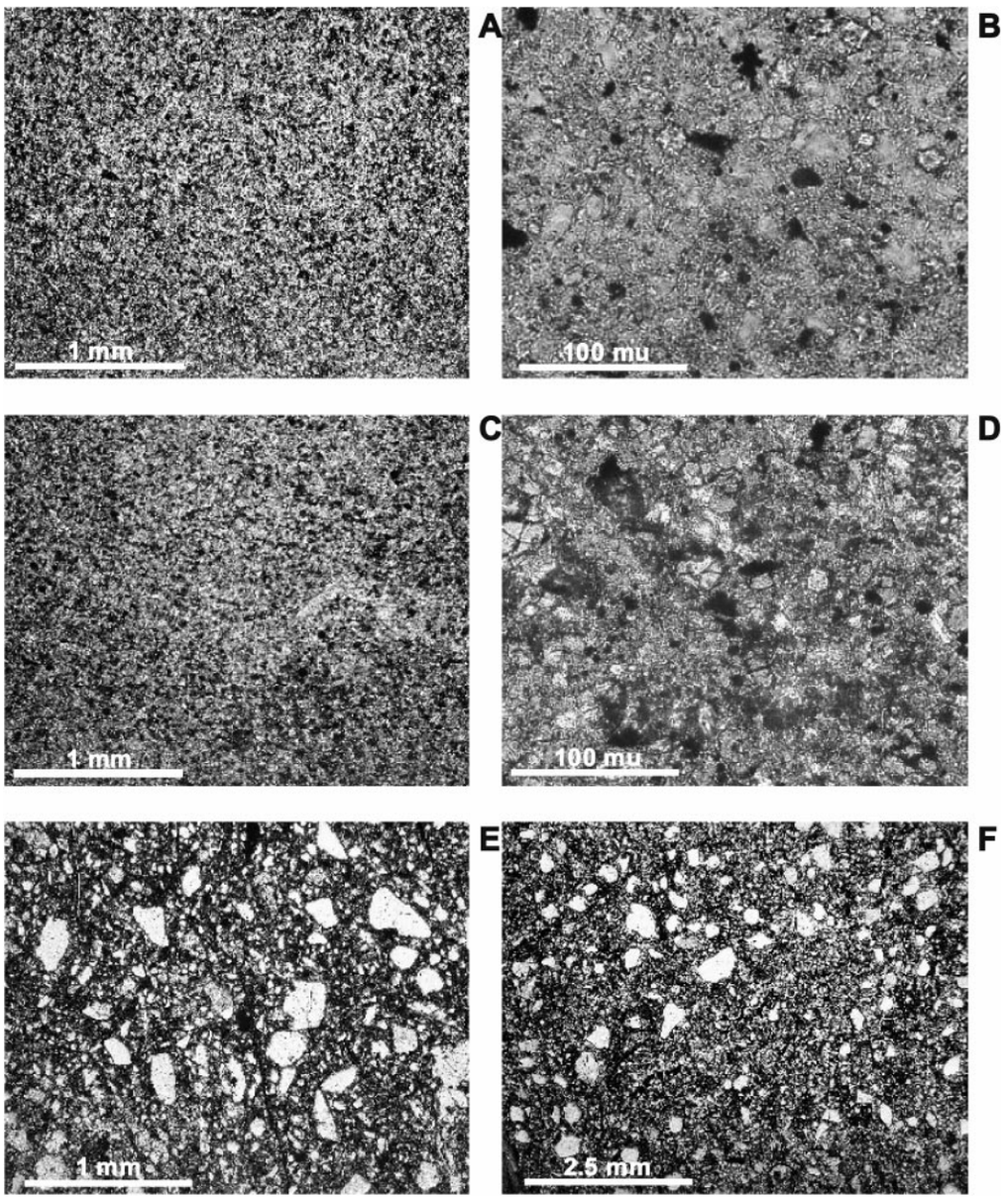

FIG. 6. Photomicrographs of typical sediment fabrics (see Figure 5 for location in contoured velocity diagram). (a) Nearly pure lime mudstone with sponge spicules and minor quartz grains. (b) Argillaceous lime mudstone with fine silt-size quartz (sample 191). (c) Argillaceous lime mudstone with fine silt-size quartz (sample 151). (d) Carbonaceous quartz (angular) sandstone (sample 89). (e) Carbonaceous quartz siltstone (sample 9). (f) Carbonaceous quartz siltstone (sample 191). (g, h) Carbonaceous quartz siltstone or wackestone (sample 179). (i, j) Carbonaceous quartz siltstone with peloidal grains or wackestone (sample 103). (k) Fine-grained siltstone with minor amounts of carbonate cement (sample 189). (l) Shale with less than 10% carbonate material (sample 76). See text for discussion.

compaction is less than that generally observed in shales that were buried to several kilometers. However, as shale velocities are comparable, possibly minor amounts of carbonate contribute to the acoustic properties of the shales studied.

Mineralogical and textural parameters

The primary control on acoustic velocity and impedance within the data set is porosity (and density). Mineralogy and grain size control the remainder of the variation. All ternary diagrams shown in Figure 5 suggest that the influence of clay content progressively increases with decreasing carbonate content. A sharp change in acoustic properties seems to occur in the range of 10% to 20% clay content. Similarly, a rapid change in acoustic properties relates to a carbonate content change at around 30–40% for shaley sediments and 15–20% for quartz arenites. As a result, there are no clear thresholds defining abrupt changes in physical properties as a function of mineralogical and textural composition. In other words, the position, orientations within the ternary diagram, and steepness of the slope of the changing physical properties as a function of the textural/mineralogical parameters vary. It should be noted that the significant changes in acoustic properties in this particular data set do overlap in part with traditional classification boundaries (such as, for example, the change from grain to mud supported) that were also used by Vernik and Nur (1992). However, they are strongly overprinted by the effect of carbonate in particular form (shells and shell debris) and as a

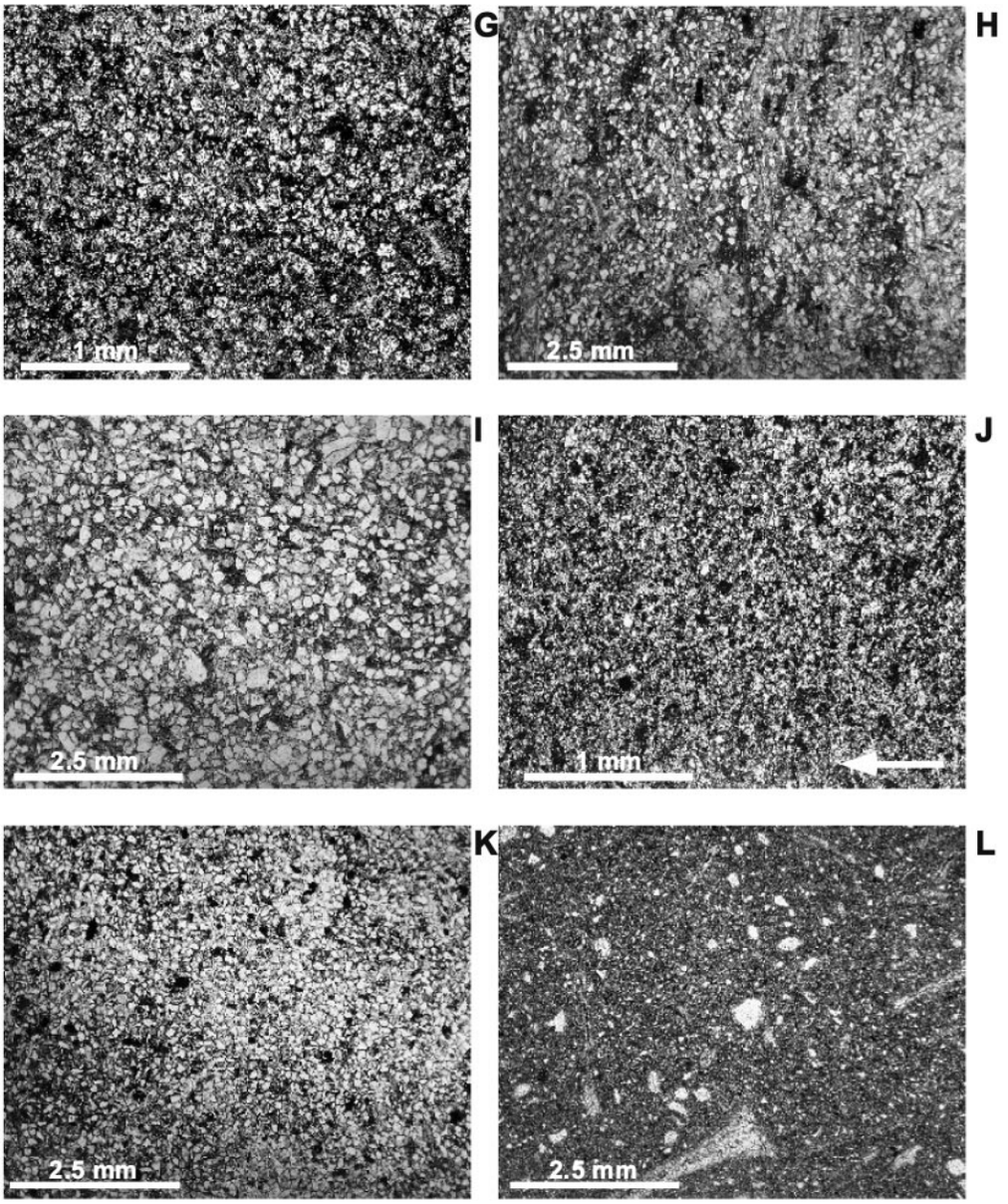

FIG. 6. *Continued.*

diagenetic product. The presence of carbonate cement is probably strongly related to the high variation in acoustic properties versus the low variation in the clay-dominated sediments. This phenomenon has been earlier documented for pure carbonates (Anselmetti et al., 1997; Kenter and Ivanov, 1995).

The general negative effect of clay on the acoustic properties of quartz arenites has been previously noted (Wyllie et al. 1956, 1958; Raymer et al., 1980; Tosaya and Nur, 1982; Kowallis et al., 1984; Han et al., 1986). Nur and Vernik (1992) expanded on this relationship and used the ternary classification diagram of sandstones (after Greensmith, 1989) to study the effect of grain size, grain fabric, and clay content on the acoustic properties of siliciclastics. In addition, they addressed the influence of diagenesis on porosity reduction and velocity increase. Although their study is semiquantitative and assessments of the quantity of clay and fabric were based on petrographic observations, it is an excellent attempt to link geological parameters to ultrasonic, and eventually seismic-scale, acoustic properties. Even though the data sets are difficult to compare, semiquantitative, and lacking significant amounts of carbonate material, there seems to be a significant difference in their velocity trends and those in our data. The porosity-velocity relationship in the Vernik and Nur (1992) data set implies a nearly linear relationship, whereas our data set, for the noncarbonate part, clearly display a nonlinear trend and generally lower velocities at a given porosity (Figure 3). The reasons for this are as yet unclear but could be related to differing compaction histories and possibly higher amounts of carbonate (diagenesis) in the quartz arenites in the Vernik and Nur (1992) data set than detectible by standard petrography.

Klimentos and McCann (1990), Stafleu et al. (1994), and Kenter and Ivanov (1995) documented a similar clay effect in carbonates, which are more susceptible to diagenesis and hence more complicated than siliciclastics from a petrophysical point of view (e.g., Rafavich et al., 1984; Anselmetti et al., 1997; Klimentos and McCann, 1990; Kenter et al, 1997a). As the ultimate goal is to link geological properties (the depositional process) to intrinsic ultrasonic and seismic velocities, it is crucial to acquire quantitative measurements of textural and mineralogic parameters. Especially because they have nonlinear relationships with acoustic properties and carbonate diagenesis plays an important role, traditional classification schemes do not explain the variation in acoustic properties.

CONCLUSIONS

This study is based on quantitative measurements of mixtures of three textural and mineralogical parameters (clay, silt/sand, and carbonate) in more than 200 plug samples from outcrop and nearby, boreholes. Two of these parameters are clearly defined: clay and silt/sand. However, the carbonate fraction contains aspects of not only textural and mineralogical character, but also has a strong diagenetic component. Since the quantitative data allows the observation of

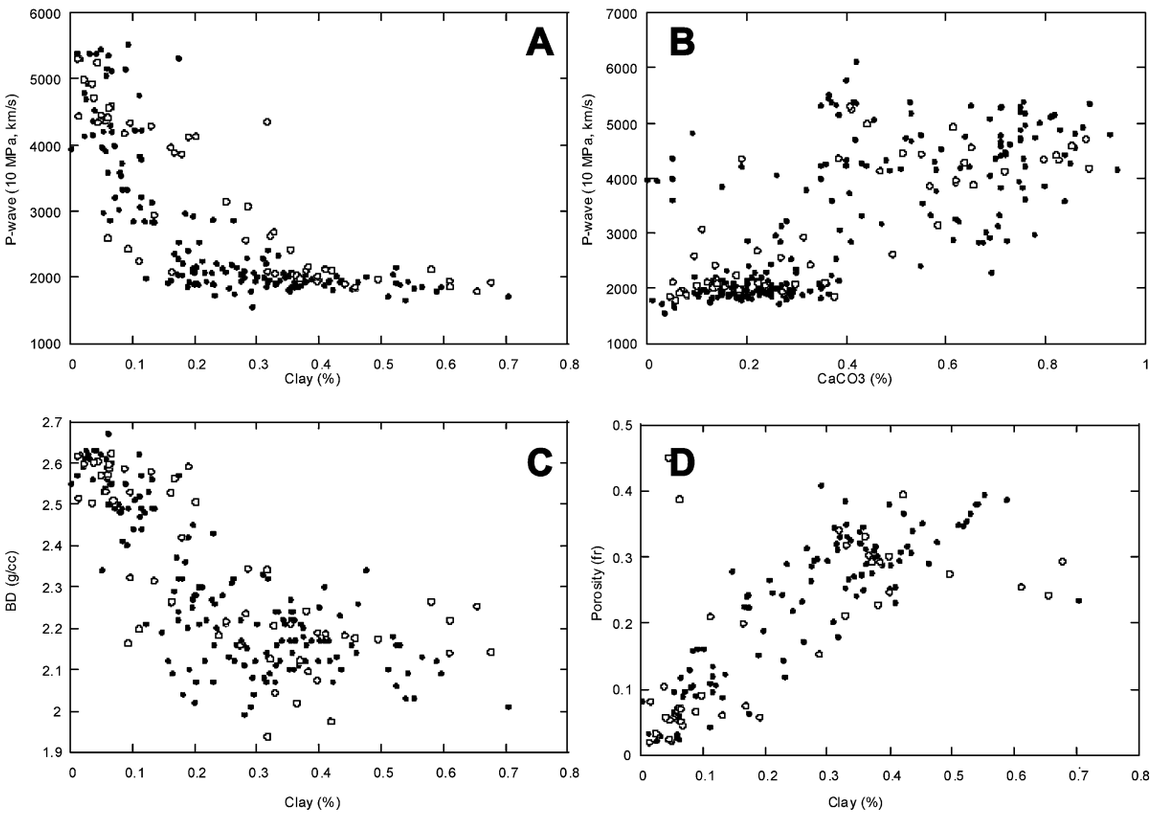

FIG. 7. Crossplots of terminal water-saturated P-wave velocities versus clay content (a) and carbonate content (b) for the total data set of 228 plug samples. Crossplots of bulk density and porosity versus clay content (c and d, respectively) confirm general relationships between pore space and clay in sedimentary rocks. See text for discussion.

four-dimensional relationships in contoured ternary diagrams, the following important relationships were established.

Primary control on the acoustic properties is exerted by porosity. The remaining variation in acoustic properties is explained by the mineralogical and textural parameters: clay (fraction <8 μm), silt/sand (fraction >8 μm), and carbonate particular material and cement. No clear linear thresholds are defined; however, a general trend is that clay and carbonate content have opposite and overlapping effects on acoustic properties. The influence of clay content progressively increases with decreasing carbonate content and visa versa. In addition, with increasing carbonate content the variation of acoustic velocity at a given porosity value increases to nearly twice of that in the clay-dominated sediment. Traditional classification boundaries, such as the change from grain to mud supported, are present but strongly overprinted by this interplay between clay and carbonate. No attempt yet has been made to distinguish the occurrence of granular, detrital carbonate from chemical, diagenetic carbonate.

The results of this quantitative analysis may have important implications for the prediction of porosity from acoustic velocities in similar mixtures of sediment. In addition, they may provide a direct link between acoustic properties and the primary depositional system and sequence stratigraphic history of the studied interval, thereby connecting geology and seismics.

ACKNOWLEDGMENTS

We thank Nanda Koot and Volker Wiederhold for their assistance in preparing the rock plugs and thin sections. Bruis Gianotten is acknowledged for operating the petrophysics laboratory. Bryan van der Bilt is thanked for lab measurements and assisting with the core descriptions. Reviews by Wolfgang Schlager and David Smeulders substantially improved the quality of the final manuscript. This research is a joint effort of the Integrated Solid Earth Sciences Program (ISES) and the Projet "Image Sismique et Sédiments" between the French Science Foundation (CNRS), the Ifremer Oceanographic Research Institute, and TotalFinaElf (TFE). The Industrial Associates Program of Wolfgang Schlager provided important financial support for this study.

REFERENCES

Anselmetti, F. S., Eberli, G. P., and Bernoulli, D., 1997, Seismic modeling of a carbonate platform margin (Montagna della Maiella, Italy): Variations in seismic facies and implications for sequence stratigraphy, *in* Marfurt, K. J., and Palaz, I., Eds., Carbonate seismology: Soc. Expl. Geophys., 373–406.

Bourbie, T., Coussy, O., and Zinszner, B., 1987. Acoustics of porous media: Editions Technip.

Bracco Gartner, G. L., and Schlager, W., 1997, Topographic slope as an estimator of acoustic impedance: Sedimentary Geology, **112**, 1–6.

Carmichael, R. S., 1990, Practical handbook of physical properties and minerals: CRC Press.

Cornford, C., 1984, Source rocks and hydrocarbon of the North Sea, *in* Glennie, K. W., Ed., Introduction to the petroleum geology of the North Sea: Blackwell Scientific Publ., 171–204.

Domenico, S. N., 1977, Elastic properties of unconsolidated porous sand reservoirs: Geophysics, **42**, 1339–1368.

Dvorkin, J., and Nur, A., 1998, Time-average equation revisited: Geophysics, **63**, 460–464.

El Albani, A., Deconinck, J. F., Herbin, J. P., and Proust, J. N., 1993, Caracterisation geochimique de la matiere organique et mineralogie des argiles du Kimmeridgien du Boulonnais: Ann. Soc. Geol. Nord, **2**, 113–120.

Gallois, R. W., 1976, Coccolithic blooms in the Kimmeridge Clay and origin of North Sea oil: Nature, **259**, 473–475.

Gardner, G. H. F., Gardner, L. W., and Gregory, A. R., 1974. Formation velocity and density, the diagnostic basis for stratigraphic traps: Geophysics, **39**, 770–780.

Geyssant, J. R., Vidier, J., Herbin, J., Proust, J. N., Deconinck, J. F., 1993, Biostratigraphie et paléoenvironnement des couches de passage Kimméridgien/Tithonien du Boulonnais: Nouvelles données paléontologiques (ammonites), organisation séquentielle et contenu en matière organique : Géologie de France, **4**, 11–24.

Greensmith, J. T., 1989, Petrology of sedimentary rocks: Unwin Hyman.

Han, D., Nur, A., and Morgan, D., 1986, Effects of porosity and clay content on wave velocities in sandstones: Geophysics, **51**, 2093–2107.

Herbin, J. P., Geyssant, J. R., Melieres, F., Muller, C., Penn, I. E., and Yorkim, G., 1993, Variation of the distribution of organic matter within a transgressive system tract : Kimmeridge Clay (Jurassic), England, *in* Katz, B., and Pratt, L., Eds., Petroleum source rocks in a sequence stratigraphic framework: Am. Assn. Petr. Geol., 67–100.

Jankowsky, W., 1970, Empirical investigation of some factors affecting elastic wave velocities in carbonate rocks: Geophys. Prosp., **18**, 103–118.

Kenter, J. A. M., Fouke, B. W., and Reinders, M., 1997a, Effects of differential cementation on the sonic velocities of upper creataceous skeletal grainstones (southeastern Netherlands): J. Sedimentary Res., **67**, 178–185.

Kenter, J. A. M., and Ivanov, M., 1995, Parameters controlling acoustic properties of carbonate and volcaniclastic sediments at sites 866 and 869, *in* Winterer, E. L., Sager, W. W., and Sinton, J. M., Eds., 1995, Proc. Ocean Drilling Program, Scientific Results, **143**, 305–316.

Kenter, J. A. M., Podladchikov, F. F., Reinders, M., Van der Gaast, S. J., Fouke, B. W., and Sonnenfeld, M. D., 1997b, Parameters controlling sonic velocities in a mixed carbonate-siliciclastics Permian shelf-margin (upper San Andres Formation, Last Chance Canyon, New Mexico): Geophysics, **62**, 505–520.

Klimentos, T., and McCann, C., 1990, Relationships among compressional wave attenuation, porosity, clay content, and permeability in sandstones: Geophysics, **55**, 998–1014.

Konert, M., and Vandenberghe, J., 1997, Comparison of laser grain size analysis with pipette and sieve analysis: A solution for underestimation of the clay fraction: Sedimentology, **44**, 523–535.

Kopf, M., 1979, Die teufenabhängigkeit der petrophysikalischen parameter dichte, geschwindighkeit, schallharte und reflexionskoeffizient: Geophysik und Geologie, **2**, 125–133.

Kowallis, B. J., Jones, L. E. A., and Wang, H. F., 1983, Velocity-porosity-clay content systematics of poorly-consolidated sandstones: EOS, **64**, 863.

Mahieux, G., Proust, J. N., Tessier, B., and De Batist, M., 1998, High resolution seismic and sequence stratigraphy: Relationships between the seismic record and the sequence stratigraphic picture: Marine Petr. Geol., **15**, 329–342.

Mahieux, G., Proust, J. N., Tessier, B., De Batist, M., and Chamley, H., 1999, Stratigraphie sismique et séquentielle haute résolution des formations du Jurassique supérieur du Boulonnais (Nord de la France): C. R. Acad Sci. Paris, **328**, 341–346.

Nafe, J. E., and Drake, C. L., 1963, Physical properties of marine sediments, *in* Hill, M. N., Ed., The Sea: The Earth beneath the sea (and) history: Wiley-Interscience, **3**, 794–815.

Prins, M. A., and Stuut, J. B., 1999. Evaluation of the Malvern 2600 laser-diffraction size analyzer for use with fine-grained sediments, *in* Prins, M. A., Ed., Pelagic, hemipelagic and turbidite deposition in the Arabian sea during the late Quarternary: Utrecht University, Thesis, **168**.

Prins, M. A., and Weltje, G. J., 1999, End-member modeling of siliciclastic grain-size distributions of sediment mixtures: PhD thesis, Vrije Universiteit, Amsterdam.

Prothero, D. R., and Schwab, F., 1996, Sedimentary geology: An introduction to sedimentary rocks and stratigraphy: W. H. Freeman and Co.

Proust, J. N., Deconinck, J. F., Geyssant, J. R., Herbin, J., and Vidier, J. P., 1993, Nouvelles données sédimentologiques dans le Kimméridgien et le Tithonien du Boulonnais France: C. R. Acad Sci Paris, **316**, 363–369.

———1995, Sequence analytical approach to the upper Kimmeridgian–lower Tithonian storm-dominated ramp deposits of the Boulonnais (northern France): A landward time equivalent to offshore marine source rocks: Geologische Rundschau, **84**, 255–271.

Proust, J. N., Mahieux, G., and Tessier, B., 2001, Field and seismic images of sharp-based shoreface deposits: Implications for sequence stratigraphic analysis: J. Sedimentary Res, **71**, 944–957.

Rafavich, F., Kendall, C. H. St. C., and Todd, T. P., 1984, The relationship between acoustic properties and the petrographic character of carbonate rocks: Geophysics, **49**, 1622–1636.
Raymer, L. L., Hunt, E. R., and Gardner, J. S., 1980, An improved transit-to-porosity transform: 21st Ann. Logging Symp., Soc. Prof. Well Log Analysts, 1–12.
Stafleu, J., Everts, A. J. W., and Kenter, J. A. M., 1994, Seismic models of a prograding carbonate platform: Vercors, SE France: Marine Petr. Geol., **11**, 513–527.
Tosaya, C., and Nur, A., 1982, Effect of diagenesis and clays on compressional velocities in rocks: Geophys. Res. Lett., **9**, 5–8.
Vernik, L., and Nur, A., 1992, Petrophysical classification of siliciclastics for lithology and porosity predictions from seismic velocities: AAPG Bull., **76**, 1295–1309.
Wang, Z., and Nur, A., 1992, Seismic and acoustic velocities in reservoir rocks; **2**: Theoretical and model studies: Soc. Expl. Geophys.
Williams, P. F. V., 1986, Petroleum geochemistry of the Kimmeridge Clay on onshore southern and eastern England: Marine Petr. Geol., **3**, 258–281.
Wyllie, M. R. J., Gregory, A. R., and Gardner, G. H. F., 1956, Elastic wave velocities in heterogeneous and porous media: Geophysics: **21**, 41–70.
———1958. An experimental investigation of factors affecting elastic wave velocities in porous media: Geophysics, **23**, 459–493.